# Estimated solar-neutrino capture rates of $^{131}$Xe: Implications for multi-tonne Xe-based experiments

**J Kostensalo and J. Suhonen**

University of Jyväskylä, Department of Physics, 40014 Jyväskylä,Finland

E-mail: joel.j.kostensalo@student.jyu.fi

**K Zuber**

Institut für Kern- und Teilchenphysik, TU Dresden, Zellescher Weg 19, 01062 Dresden, Germany

E-mail: kai.zuber@tu-dresden.de

**Abstract.** Various large-scale experiments for double beta decay or dark matter are based on xenon. Current experiments are on the tonne scale, but future ideas also aim for even larger sizes. Here we study the potential of the isotope $^{131}$Xe to allow real-time capture measurements of solar *pp*-chain neutrinos, besides classical neutrino-electron scattering. Here we use improved nuclear-structure calculations to determine the cross sections of solar neutrinos on $^{131}$Xe . Our updated capture-rate estimate is $(80 \pm 22)$ SNU, with neutrino survival probabilities taken into account. According to our calculations, the $^{8}$B neutrinos are the dominant contribution to the total capture rate. Due to our more accurate treatment of the phase-space factor the computed capture rate, $(60 \pm 19)$ SNU, is significantly larger than what was expected based on previous calculations. This improves considerably the prospects of real-time monitoring of *pp*-chain neutrinos for long periods of time.

## 1. Introduction

Neutrinos play a crucial role in modern particle, nuclear and astrophysics, including cosmology [1, 2]. It has been a major achievement of the last 25 years to show that neutrinos have a non-vanishing rest mass and that the problem of missing solar neutrinos could be solved [3, 4]. Solar-neutrino measurements are one of the most important ingredients for the understanding of the Sun, especially for the nuclear-fusion processes. The low-energy region, below 1 MeV, of solar neutrinos has been observed in various radiochemical experiments starting from the famous Homestake experiment [5] and continuing further to radiochemical experiments based on $^{71}$ Ga, namely GALLEX [6], GNO [7, 8] and SAGE [9], which were able to enter the energy region of the most abundant *pp* neutrinos. All of these measurements were radiochemical approaches using a counting method, without any energy or time information.

The first real-time detection measurement of solar neutrinos was performed by Kamiokande [10], which is a water Cherenkov detector. The observed signal is the Cherenkov light which could be used for energies above about 3.5 MeV. Hence, the observed neutrinos are dominantly coming from $^{8}$B. This experiment improved data taking over several decades by building a larger detector in the form of Super-Kamiokande, and it also kept reducing backgrounds continuously [11]. Another milestone experiment was the one of the Sudbury Neutrino Observatory (SNO) [12], which measured for the first – and still only time – the total solar-neutrino flux [3]. Based on all these data it was possible to show that neutrinos are oscillating and that matter effects are at work.

By using neutrino-electron scattering, the large-scale liquid scintillator experiment KamLAND was able to measure solar $^{7}$Be [13] and $^{8}$B [14] neutrinos real-time. The most relevant measurements in the last decade for solar neutrinos have been performed by the Borexino experiment, based on the same detection method. In addition, Borexino not only measured the *pep* flux [15], but also the fundamental *pp*-neutrinos [16], and was finally able to achieve a common fit using *pp*, *pep*, and $^{7}$Be neutrinos [17]. Last but not least, Borexino has recently observed neutrinos from the CNO cycle, which brought the decades-old prediction of Bethe into reality [18].

Despite of all these major improvements and discoveries there is still a desire to perform real-time experiments in the low-energy region of solar neutrinos, especially for the fundamental *pp* neutrinos. However, in spite of the success of all the above-mentioned experiments, special dedicated solar-neutrino experiments will likely not be performed anymore. Nevertheless, potential improvements on solar neutrino data can still be done in a parasitic way. The related experiments are linked to astro-particle and nuclear physics which - among others - include topics like searches for dark matter or neutrinoless double beta decay. As neither of these two have been observed, experiments have to push towards larger and larger masses for a potential discovery. Thus, next-generation multi-tonne-scale experiments, looking for double beta decay and searching for dark matter, will appear and they even might suffer from interference with solar

neutrinos. On the positive side, this might allow to gain more information about solar neutrinos.

Here we want to explore the potential of the new large-scale xenon-detector experiments [19] for real-time *pp*-chain solar-neutrino detection. These kind of experiments are detecting also solar neutrinos via neutrino-electron scattering – like scintillators – and produce recoil electrons. Here we focus on the xenon isotope $^{131}$Xe , which has a natural abundance of 21.2% and a threshold of 355 $\pm$5 keV [20] for neutrino capture. Consequently, it is able to cover the highest 65 keV of the *pp*-neutrinos, up to the endpoint of 420 keV. Hence, an additional neutrino reaction, besides electron-neutrino scattering, is possible via the neutrino-capture reaction

$$\nu_e + {}^{131}\mathrm{Xe}(3/2^+_{\mathrm{gs}}) \rightarrow {}^{131}\mathrm{Cs}(J^\pi) + e^-, \tag{1}$$

where $J^\pi$ symbolizes the spin-parity of the final states in $^{131}$Cs. Unfortunately, no nice coincidence can be formed as the half-life of $^{131}$Cs is 9.69 days. The detection signal of $^{131}$Cs would be X-rays of about 30 keV and Auger electrons around 3.4 and 24.6 keV. Such a long time spread prohibits a meaningful coincidence. The only way out of this situation would be based on the accumulation of $^{131}$Cs and a subsequent sophisticated analysis of the low-energy spectrum. This might allow to identify a kind of peak by integrating the number of daughter decays.

## 2. Neutrino cross section

The neutrino-nucleus cross-section calculations presented here are based on the Donnelly-Walecka method [21, 22] for the treatment of semi-leptonic processes in nuclei. The necessary formulae and details of the application of the formalism can also be found in [23].

Given that the threshold for the neutrino-capture reaction on $^{131}$Xe is 355 $\pm$5 keV, we need to calculate the shell-model final states up to about 1.4 MeV in order to cover neutrino energies up to 1.75 MeV, which is sufficient for *pp*, *pep*, $^7$Be and CNO neutrinos. The *hep* and $^8$B neutrinos are treated by using the microscopic quasiparticle-phonon model (MQPM), and the related calculations are described later in the text. The initial and final states for these transitions, as well as the one-body transition densities, were calculated in the shell-model framework using the computer code NuShellX@MSU [24]. The calculations were done in a model space consisting of the orbitals $0g_{7/2}$, $1d$, $2s$ and $0h_{11/2}$, for both protons and neutrons, with the effective Hamiltonian sn100pn [25]. Due to the huge computational burden of the shell-model calculations, some truncations had to be made. For the states $1/2^+_1$, $3/2^+_{1,2}$, and $5/2^+_{\mathrm{g.s.},2}$ the neutron orbital $0f_{7/2}$ was filled with 8 neutrons, while no restrictions were posed on the other orbitals. However, the computational burden of this truncation was too large to allow calculations of more states. Instead, a second calculation was done keeping additionally the proton orbital $0h_{11/2}$ empty. This was done for 50 states of the spin parities $1/2^\pm, 3/2^\pm, 5/2^\pm, 7/2^-$ in $^{131}$Cs. The ground state of $^{131}$Xe was calculated in both cases with the same truncation

as used for $^{131}$Cs in order to keep the calculations consistent. For the low energies considered here, the higher-multipole contributions are more than an order of magnitude smaller, and thus the higher-spin states are not relevant. The negative-parity states correspond to first-forbidden transitions, which at few MeV energies are expected to be suppressed by a couple orders of magnitude with respect to the allowed transitions. On the other hand, a transition to e.g. a $7/2^+$ state would be second-forbidden, which brings in a suppression by couple orders of magnitude with respect to the first-forbidden transitions. In addition, the computational requirements for the spins 7/2 and 9/2 are much greater than for the lower spins and thus it was not computationally feasible to include any more high-spin transitions.

For $^8$B and *hep* neutrinos we adopt the recent cross-section results of Pirinen et al. [26], which are calculated using the earlier-mentioned MQPM [27, 28]. MQPM is an extension of the quasiparticle random-phase approximation to odd-mass nuclei. The MQPM approach can utilize a much larger model space than the shell model and thus for higher-energy neutrinos it is a good choice, while for the individual low-energy states the shell model is preferable.

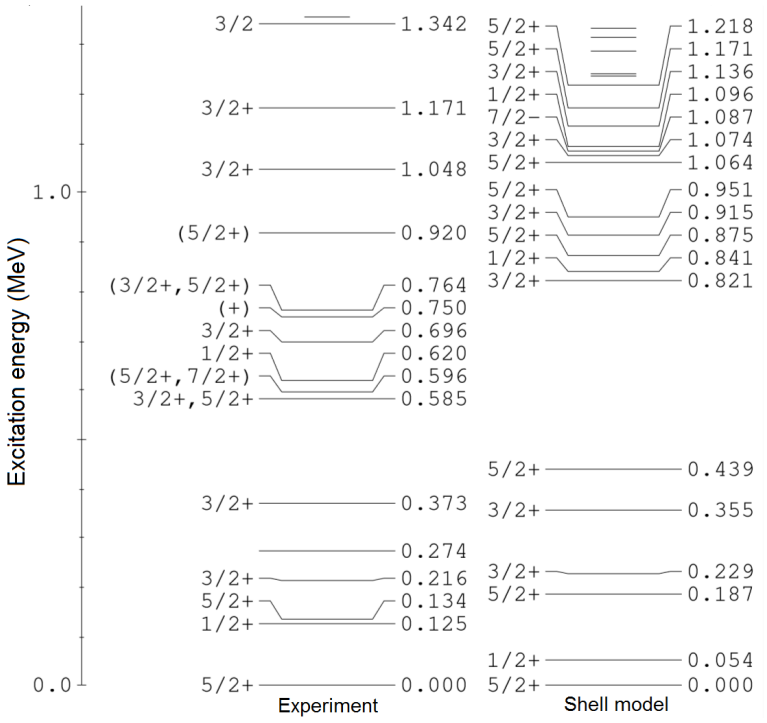


**Figure 1.** Experimental and shell-model calculated energy spectra for $^{131}$Cs, with only the states relevant for the neutrino capture on the $3/2^+$ ground state of $^{131}$Xe included in the computed spectrum.

The shell-model-calculated energy spectrum of $^{131}$Cs is presented in figure 1. The shell model manages to predict the ground-state spin-parity correctly, and it also predicts the set of states below half an MeV quite accurately. However, there is a large gap, larger than in the experimental spectrum, between the set of lowest states

and the next six states. The influence of this gap on the cross-section and capture calculations will be discussed later in the text. Since the exact energies are important for the lowest-energy states, we adopt the experimental energies for the excited states $1/2^+_1$, $3/2^+_{1,2}$ and $5/2^+_2$. While the individual-state contributions for the higher states may have large uncertainties associated with them, these uncertainties can be expected to average out to a significant degree (some contributions being too large, some too small), given that a significant number of the states appears not to be missing. Thus, there is no reason to expect that the excited-state contributions would be systematically too small or large.

Furthermore, the ground-state-to-ground-state scattering cross section can be deduced from the electron-capture half-life of $^{131}$Cs through the reduced transition probability $B(\mathrm{GT})$, obtained from

$$B(\mathrm{GT}) = \frac{2J+1}{2J'+1}\frac{2\pi^3\hbar^7 \ln 2}{m_e^5 c^4 (G_\mathrm{F}\cos\theta_\mathrm{C})^2} \times 10^{-\log ft} = 0.0178, \qquad (2)$$

where $J = 5/2$ is the spin of the $^{131}$Cs ground state, $J' = 3/2$ is the spin of the $^{131}$Xe ground state, $\theta_\mathrm{C} \approx 13.04^\circ$ is the Cabibbo angle, $G_\mathrm{F}$ is the Fermi coupling constant and $t$ is the electron-capture half-life. The value of the phase-space factor $f = 5.548$ can be interpolated from the tables of Ref. [29]. For the rest of the states we adopt an effective value $g_\mathrm{A} = 1.0$ of the axial-vector coupling in order to account for the limited model space (see e.g. the review [30]).

In the paper of Pirinen *et al.* [26] the MQPM results for $^8$B neutrinos are given for $g_\mathrm{A}$ values of 0.7 and 1.0. We choose the value $g_\mathrm{A} = 1.0$ here but fix the ground-state-to-ground-state cross section using the half-life of $^{131}$Cs, as was done in the case of the shell-model calculations.

The computed cross sections as functions of the neutrino energy have been presented for the shell model and for the MQPM in Fig. 2. For the energies relevant for *pp*, *pep*, $^7$Be and CNO neutrinos, the cross section is dominated by the ground-state-to-ground-state contribution, while for $^8$B and *hep* neutrinos the excited states dominate. The individual-state contributions for the shell model have been discussed in the recent article [31]. Most of the excited-state contribution for *pp*, *pep*, $^7$Be, and CNO neutrinos is expected to come from the $5/2^+$ state at 134 keV, while the $3/2^+$ states at 216 keV and 373 keV contribute each about 20% of the 134 keV state contribution. The contribution from the $1/2^+$ state at 125 keV is significantly suppressed with respect to the other excited states. The rest of the excited states have much smaller individual contributions due to phase-space limitations. For MQPM the individual states have been discussed in Pirinen *et al.* [26] for the dominant $^8$B neutrinos. Here, the low-lying states contribute very little while the majority of the contribution comes from several $3/2^+$ and $5/2^+$ states between 3 MeV and 8 MeV.

The contributions for each component of the neutrino spectrum are given in Table 1. By far the largest contribution, 77%, comes from the $^8$B neutrinos. The *pp* and $^7$Be contributions are of the same order of magnitude, and together they contribute some 19% to the total capture rate. Thus, calculating the solar-neutrino spectrum only for $^8$B

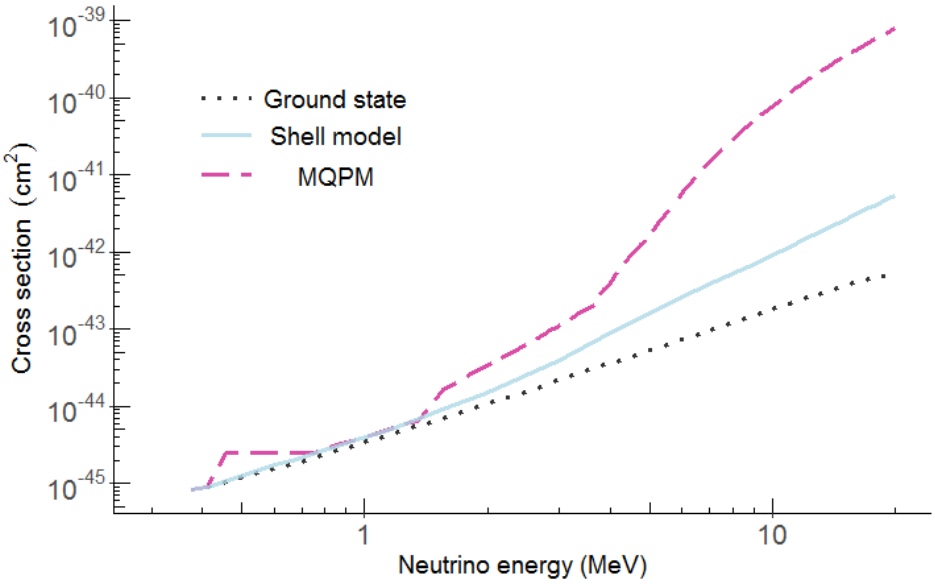


**Figure 2.** Theoretical neutrino-nucleus cross section based on our shell-model calculation and the MQPM calculation of Pirinen *et al.* [26]. The ground-state contribution can be related to the $^{131}$Cs half-life and is thus known to few tenths of per cent. The *pp*, *pep*, $^{7}$Be and CNO contributions are calculated using the shell-model cross sections. The maximum energy of these neutrinos is about 1.75 MeV. The $^{8}$B and *hep* contributions are calculated using the MQPM which is able to take into account the excited states at higher energies.

**Table 1.** The nuclear-structure model, survival probability and the total neutrino flux (in units of cm$^{-2}$s$^{-1}$), adopted for each component of the solar-neutrino spectrum. The fluxes are from the solar model BS05(OP) [32] and survival probabilities from [33]. The last two lines give the solar-neutrino capture rates of the present work and Georgadze *et al.* [34] in units of SNU.

| | *pp* | *pep* | *hep* | $^{7}$Be | $^{8}$B | $^{13}$N | $^{15}$O | $^{17}$F |
|---|---|---|---|---|---|---|---|---|
| Theory | SM | SM | MQPM | SM | MQPM | SM | SM | SM |
| Surv. | 0.54 | 0.5 | 0.36 | 0.54 | 0.36 | 0.54 | 0.5 | 0.5 |
| Total flux | $5.99\times10^{10}$ | $1.42\times10^{8}$ | 7930 | $4.84\times10^{9}$ | $5.69\times10^{6}$ | $3.07\times10^{8}$ | $2.33\times10^{8}$ | $5.84\times10^{6}$ |
| SNU (new) | 4.47(9) | 1.9(4) | 0.33(10) | 11.4(17) | 62(19) | 0.62(7) | 1.3(3) | 0.035(8) |
| SNU [34] | 5.2 | 0.80 | - | 9.6 | 4.6 | 0.86 | 0.90 | - |

neutrinos, as done in Ref. [26], results in a notable under prediction of the total number of events. The role of the individual components in experiments has been discussed recently in [35] in the context of the DARWIN experiment.

While the ground-state-to-ground-state contribution (which is 15.2 % of the total cross section) is known very precisely, with an uncertainty estimated here as 2 % due to the precision of the natural constants and the phase-space factor $f$, there are quite large uncertainties related to the other states. The uncertainties related to the excited-state contributions pertain to the nuclear-structure description of the low-lying states for the low-energy solar neutrinos and higher-lying states for the *hep* and $^{8}$B neutrinos,

in addition to the uncertainties in the value of the axial coupling $g_{\rm A}$ for the (higher) excited states. One can test the effect of the low-lying states by shifting by hand the shell-model-computed energies of the six states lying above the theoretical energy gap. A shift of these states, originally between 0.821 MeV and 1.064 MeV in Fig. 1, down by some 236 keV yields a theoretical spectrum which matches well the experimental one. The effect of this shift on the capture rates is as follows: For *pp* neutrinos there is no effect (the shifted levels are too high in energy), for *pep* neutrinos the change is +0.720 SNU, $^{7}$Be neutrinos +1.00 SNU, for $^{13}$N neutrinos +0.096 SNU, for $^{15}$O neutrinos +0.441 and for $^{17}$F neutrinos +0.011 SNU, all together +2.27 SNU. The effects of the shifted spectrum on the capture rates have been taken into account in the numbers and their error estimates in the fourth row of Table 1. For the higher-energy neutrinos, *hep* and $^{8}$B, the effect is negligible. Concerning the value of the axial coupling, based on the review [30], it is clear that a quenched value, i.e. smaller than the free-nucleon value 1.27, must be used. For the low-value side of the $g_{\rm A}$ range, a heavily quenched value $g_{\rm A} = 0.7$ has been considered in [26]. This would correspond to an extreme scenario for the lower bound. Thus, a reasonable range for $g_{\rm A}$ would be 0.7–1.3. For the cross section (which is roughly proportional to $g_{\rm A}^2$) this would correspond to 49 - 169 % of the best estimate. Assuming this to be a 95 % confidence interval, the $1\sigma$ uncertainty would correspond to about 30 %. Assuming this 30 % uncertainty, independent of the ground-state uncertainty, for the states other than the ground state, the total solar-neutrino capture rate for $^{131}$Xe amounts to

$$R(^{131}\mathrm{Xe}) = (80 \pm 22)\ \mathrm{SNU}, \qquad \text{(Solar neutrinos)} \tag{3}$$

which has been corrected for the survival probabilities from [33], and which is much larger than the old estimate 20.0 SNU of Georgadze *et al.* [34]. The *pp*-neutrino capture rate is predicted to be about 14 % lower than the previous estimate. About 4 % of this difference is explained by the updated interpolation of the $logft$-value, 0.5 % by the updated flux in the new solar model, and the rest is due to the contributions from the excited states. For $^{7}$Be neutrinos the estimate for the rate is increased with respect to the previous results, owing to the increased $^{7}$Be neutrino-flux estimate in the more recent solar model [32]. However, the results are practically in agreement within the uncertainties. The major difference in the rates relates to $^{8}$B neutrinos, which in our updated calculations are predicted to contribute over 10 times as many counts as in the old work. The reason for this vast difference is unclear since in [34] the authors give no information about the details of their nuclear-structure calculations or their computed scattering cross sections. It seems that some important contributions to the cross sections have been missed in their calculations, in particular in the $3 - 8$ MeV excitation region in $^{131}$Cs (see [26], Fig. 6, bottom-right panel). This difference between the previous and updated estimates for the $^{8}$B neutrinos highlights how the limitations of different nuclear models can produce vastly different estimates for the cross section.

As the solar neutrino cross section is sensitive to the nuclear-structure details, a measurement of the $^{131}$Xe cross section could also be used to constrain nuclear-structure

details and thus reduce uncertainties in theoretical estimates of other weak-interaction processes in the $A \approx 130$ nuclear-mass range.

## 3. Outlook and conclusion

We have explored the potential for a solar *pp*-chain neutrino measurement by using the isotope $^{131}$Xe. Large-scale xenon detectors are used since many years for searches of dark matter and neutrinoless double beta decay. As no new physics could yet be found so far, experiments are upgraded and are now on the tonne scale, like Xenon1T [36] and LUX-ZEPLIN (LZ) [37]. Even larger detectors are planned, like the DARWIN experiment using 50 tons of Xenon [38]. Based on our calculations, the potential of real-time measurements of *pp*-chain solar neutrinos by xenon-based detectors is improved considerably due to the predicted strong contributions coming from the $^{8}$B neutrinos.

## References


[1] H. Ejiri, J. Suhonen, K. Zuber, *Phys. Rep.* **797**,1(2019).
[2] K. Zuber, *Neutrino Physics* 3rd edition, CRC Press 2020.
[3] S. N. Ahmed, *Phys. Rev. Lett.* **92**,181301(2004).
[4] B. Aharmim et al. *Phys. Rev.* **D 70**,093014(2004).
[5] B. T. Cleveland et al., *Astroph. J.* **496**,505(1998).
[6] W. Hampel et al., *Phys. Lett.* **B 447**,127(1999).
[7] M. Altmann et al., *Phys. Lett.* **B 616**,214(2005).
[8] F. Kaether et al., *Phys. Lett.* **B 685**,47(2010).
[9] J. N. Abdurashitov et al., *Phys. Rev.* C **80**,015807(2009).
[10] K. S. Hirata et al.*Phys. Rev. Lett.* **63**,16(1989).
[11] K. Abe et al., *Phys. Rev.* **D 94**,052010(2016).
[12] J. Boger et al. *Nucl. Inst. Meth. A:* **449**,172(2000).
[13] A. Gando et al., *Phys. Rev.* C **92**,055808(2015).
[14] S. Abe et al., *Phys. Rev.* C **84**,035804(2011).
[15] G. Bellini et al., *Phys. Rev. Lett.* **108**,051302(2012).
[16] G. Bellini et al., *Nature* **512**,383(2014).
[17] G. Bellini et al., *Nature* **562**,505(2018).
[18] G. Bellini et al., Nature volume 587, pages 577–582 (2020).
[19] N.Barros, J. Thurn, K. Zuber, *Journal of Physics G* **41**,115105(2014).
[20] G. Audi et al., *Chinese Phys. C* **41**,030001(2014).
[21] J. S. O'Connell, T. W. Donnelly, and J. D. Walecka, *Phys. Rev.* C **6**,719(1972).
[22] T. W. Donnelly and R. D. Peccei, *Phys. Rep.* **50**,1(1979).
[23] E. Ydrefors and J. Suhonen, Adv. High Energy Phys. **2012**, 373946 (2012).
[24] B. A. Brown, W. D. M. Rae, Nuclear Data Sheets 120 (2014) 115.
[25] B. A. Brown, N. J. Stone, J. R. Stone, I. S. Towner, and M. Hjorth-Jensen, Phys. Rev. C 71, 044317 (2005).
[26] P. Pirinen, J. Suhonen, and E. Ydrefors, Physical Review C, 99 (1), 014320 (2019).
[27] J. Toivanen and J. Suhonen, J. Phys. G. 21, 1491 (1995).
[28] J. Toivanen and J. Suhonen, Phys. Rev. C 57, 1237. (1998).
[29] N. B. Gove and M. J. Martin, Atom. Data Nucl. Data Tables 10, 205 (1971).
[30] J. T. Suhonen, Frontiers in Physics 5, 55 (2017).

[31] Scott Haselschwardt, Brian Lenardo, Pekka Pirinen, and Jouni Suhonen Phys. Rev. D 102, 072009 (2020).
[32] J. N. Bahcall A. M. Serenelli, and S. Basu, Astrophys. J. 621, L85 (2005).
[33] M. Agostini et al. (The Borexino Collaboration), Nature 562, 505 (2018).
[34] A. Sh. Georgadze, et al. *Astroparticle Physics* **953**,173(1997).
[35] J Aalbers et al. (DARWIN), Eur. Phys. J. C (2020) 80: 808.
[36] J . Aalbers et al., *Eur. Phys. J. C* **77**,881(2017).
[37] D. S. Akerib et al. *Nucl. Inst. Meth. A:* **953**,163047(2020).
[38] J. Aalbers et al., *JCAP* **11**,017(2016).